Geosci. Model Dev. Discuss., 7, 8769–8804, 2014
www.geosci-model-dev-discuss.net/7/8769/2014/
doi:10.5194/gmdd-7-8769-2014

Geoscientific Model Development Discussions
Open Access

The terminator "toy"-chemistry test: a simple tool to assess errors in transport schemes

P. H. Lauritzen[1], **A. J. Conley**[1], **J.-F. Lamarque**[1], **F. Vitt**[1], **and M. A. Taylor**[2]

[1]National Center for Atmospheric Research, Boulder, Colorado, USA
[2]Sandia National Laboratories, Albuquerque, New Mexico, USA

Received: 22 October 2014 – Accepted: 18 November 2014 – Published: 10 December 2014

Correspondence to: P. H. Lauritzen (pel@ucar.edu)

Published by Copernicus Publications on behalf of the European Geosciences Union.

Abstract

This test extends the evaluation of transport schemes from prescribed advection of inert scalars to reactive species. The test consists of transporting two reacting chlorine-like species (Cl and Cl_2) in the Nair and Lauritzen 2-D idealized flow field. The sources and sinks for the two species are given by a simple, but non-linear, "toy" chemistry. This chemistry mimics photolysis-driven processes near the solar terminator. As a result, strong gradients in the spatial distribution of the species develop near the edge of the terminator. Despite the large spatial variations in Cl and Cl_2 the weighted sum $Cl_y = Cl + 2Cl_2$ should always be preserved. The terminator test demonstrates how well the advection/transport scheme preserves linear correlations. Physics-dynamics coupling can also be studied with this test. Examples of the consequences of this test are shown for illustration.

1 Introduction

Tracer transport is a basic component of any atmospheric dynamical core. Typically transport accuracy is evaluated in ideal tests before being developed further or implemented in full models. Several tests for 2-D passive and inert transport exist in the literature (Williamson et al., 1992; Nair and Machenhauer, 2002; Nair and Jablonowski, 2008; Nair and Lauritzen, 2010). To facilitate the intercomparison of transport operators under challenging flow conditions, Lauritzen et al. (2012) proposed a standard suite of tests that was exercised by a number of state-of-the-art schemes in Lauritzen et al. (2014). These tests evaluate each advection scheme's ability to transport an inert tracer with respect to a wide range of diagnostics as well as the ability of each transport scheme to maintain non-linear tracer correlations between pairs of tracers (Lauritzen and Thuburn, 2012). While such evaluations provide useful information about the ability of each transport operator to advect inert scalars, these idealized tests do not shed

GMDD
7, 8769–8804, 2014

light on how transport methods perform under forced conditions, e.g., how the method interacts with sub-grid scale processes.

Idealized chemical processes have readily available analytic expressions for the forcing terms. The implementation of these processes as sub-grid scale forcing involves "only" solving forced continuity equations rather than the full Navier Stokes, primitive or shallow water equations that add extra levels of complexity. Indeed several simplified systems, where two species interact non-linearly, have been developed and studied quite extensively in the literature. For example, the Lotka and Voltera equations (also know as *predator-prey equations*) that are a pair of first-order, differential equations describing the dynamics of biological systems in which two species interact, one as a predator and the other as prey. For a dynamical systems analysis of the Lotka and Voltera equations, e.g., see Chapter 4 in Prigogine (1981). The equations are the same for simple chemistry systems where each chemical species is transformed to the others. A more complicated system, but also consisting of just two independent variables (and two variables held constant), is the *Brusselator* system (Prigogine and Lefever, 1968) that allows for a rich set of solutions (Prigogine, 1981). Recently Pudykiewicz (2006) coupled the Brusselator reactions to the advection–diffusion equations in a shallow water flow. The linearized system has analytic solutions (Turing, 1952) that can be used to assess the accuracy of the numerical solution to the differential equations. Pudykiewicz (2006, 2011) solved the full non-linear system, which is basically a forced advection–diffusion equation with flow prescribed from the shallow water flow solution, and examined the solutions qualitatively since the analytic solution is not known. Similar idealized systems for reactive species have been developed in the context of convective boundary layers (e.g., Kristensen et al., 2010).

The test we develop in this paper extends the Nair and Lauritzen (2010) test to two reactive species, adding one extra level of complexity while retaining the simplicity of analytic prescribed flow and known analytic solution. The inspiration for the idealized chemical reactions is photolysis-driven chemistry in which sunlight strongly influences the production and loss processes, creating very steep gradients in the individual

GMDD
7, 8769–8804, 2014

tracer distributions near the terminator boundary (as observed for chlorine species and bromine in the stratosphere; see, e.g., Anderson et al., 1991; Salawitch et al., 2009; Brasseur and Solomon, 2005). Hence these reaction coefficients lead to strong gradients coinciding with a "terminator-like" line. Another inspiration for this test is that the atomic concentration is conserved for each air parcel, while the molecular species react non-linearly with each other, e.g., total organic and inorganic chlorine in the stratosphere. So by choosing the initial condition for two tracers so that the atomic concentration is a constant throughout the domain then the atomic concentration should remain constant in space and time (as long as the chemistry exactly conserved the total chlorine). This concept is used in this test case so that an analytic solution for the atomic concentration is readily available irrespective of the complexity of the flow and non-linearity of the chemical reactions.

The paper is organized as follows. In Sect. 2 the idealized chemistry, referred to as "toy chemistry", is defined. An analysis in terms of steady-state solutions is presented. The transport operator is discussed in the context of linear tracer correlations in Sect. 3. The combination of the "toy" chemistry forcing with advection prescribed by the Nair and Lauritzen (2010) wind field (see Appendix A) defines the *terminator* test. The discrete terminator test is defined in Sect. 4 which includes a description of physics-dynamics coupling methods in the Community Atmosphere Model (CAM). Section 5 shows example solutions from the CAM Finite-Volume dynamical core (CAM-FV; Lin, 2004) and the CAM Spectral Elements dynamical core (CAM-SE; Dennis et al., 2012). In particular, the terminator test exacerbates errors associated with the preservation of linear relations and limiters as well as highlights differences in physics-dynamics coupling approaches. The summary and conclusions are in Sect. 6.

GMDD
7, 8769–8804, 2014

2 Toy chemistry

The non-linear "toy" chemistry equations for Cl_2 and Cl are

$$Cl_2 \xrightarrow{k_1} 2Cl, \tag{1}$$

$$Cl + Cl \xrightarrow{k_2} Cl_2, \tag{2}$$

where k_1 and k_2 are the rates of production of Cl and Cl_2. The reactions are designed to conserve the total number of chlorine atoms

$$Cl_y (= Cl + 2Cl_2). \tag{3}$$

The kinetic equations corresponding to the above system (Eqs. 2 and 1) are given by

$$\frac{DCl}{Dt} = 2k_1 Cl_2 - 2k_2 Cl\,Cl, \tag{4}$$

$$\frac{DCl_2}{Dt} = -k_1 Cl_2 + k_2 Cl\,Cl, \tag{5}$$

where D/Dt is the material (or total) derivative $D/Dt = \partial/\partial t + \boldsymbol{v} \cdot \nabla$ and $\boldsymbol{v}$ is the wind vector. It is easily verified that the weighted sum of Cl and Cl_2 is conserved along characteristics of the flow

$$\frac{DCl_y}{Dt} = \frac{D}{Dt}[Cl + 2Cl_2] = 0. \tag{6}$$

If the initial condition for Cl_y is constant (as we assume here), Cl_y is not a function of time and is equal to its initial value.

$$\begin{aligned} Cl_y &= Cl(t) + 2Cl_2(t), \\ &= Cl(0) + 2Cl_2(0), \end{aligned} \tag{7}$$

GMDD
7, 8769–8804, 2014

and hence,

$$\mathrm{Cl}_2(t) = \frac{1}{2}\left(\mathrm{Cl}_y - \mathrm{Cl}(t)\right). \quad (8)$$

The reaction coefficients are chosen so that k_1 is a terminator-"like" reaction coefficient mimicking the localization of photolysis (see Fig. 1) and the other reaction coefficient k_2 is constant

$$k_1(\lambda,\theta) = \max\left[0, \sin\theta \sin\theta_c + \cos\theta \cos\theta_c \cos(\lambda - \lambda_c)\right], \quad (9)$$

$$k_2(\lambda,\theta) = 1, \quad (10)$$

where λ and θ are longitude and latitude, respectively, and (λ_c, θ_c) are chosen as (20° N, 300° E) to align with the flow field. These reaction rates will produce very steep gradients in the chlorine species near the terminator. This setup is of direct application to the real atmosphere as the total chlorine in the stratosphere is conserved, while photolysis and chemical reactions partition the various components and lead to narrow gradients across the terminator.

2.1 Analytic solution for no flow

To gain more insight into the toy chemistry (and to formulate "spun-up" initial conditions), it is useful to consider the special case of no flow. For $\boldsymbol{v} = 0$ the prognostic equations for Cl and Cl_2 (Eqs. 4 and 5, respectively) can be solved analytically. Assume the reaction rates are positive (and non-zero for k_2),

$$k_1 \geq 0, \quad (11)$$

$$k_2 > 0 \quad (12)$$

and the mixing ratios are non-negative,

$$\mathrm{Cl}(0) \geq 0, \quad (13)$$

$$\mathrm{Cl}_2(0) \geq 0. \quad (14)$$

GMDD
7, 8769–8804, 2014

From the kinetic Eqs. (4) and (5) above, as well as the conservation Eq. (3) we can write

$$\frac{\mathrm{dCl}}{\mathrm{d}t} = k_1(\mathrm{Cl_y} - \mathrm{Cl}) - 2k_2\mathrm{ClCl} \tag{15}$$

Completing the square on the right-hand side leads to the expression

$$\frac{\mathrm{dCl}}{\mathrm{d}t} = -2k_2[(\mathrm{Cl} + r)^2 - D^2]. \tag{16}$$

The right-hand side can be factored, and the following partial fraction expansion can be constructed:

$$\frac{\mathrm{dCl}}{(\mathrm{Cl} + r) - D} - \frac{\mathrm{dCl}}{(\mathrm{Cl} + r) + D} = -4Dk_2\mathrm{d}t \tag{17}$$

Integration of each of these terms from time $t = 0$ to t, yields the expression

$$\ln\left(\frac{(\mathrm{Cl}(t) + r - D)(\mathrm{Cl}(0) + r + D)}{(\mathrm{Cl}(t) + r + D)(\mathrm{Cl}(0) + r - D)}\right) = -4Dk_2t, \tag{18}$$

leading to the solutions Eq. (19). The analytic solution for $\mathrm{Cl}(t)$ is

$$\mathrm{Cl}(t) = \begin{cases} D\left(\frac{(\mathrm{Cl}(0)+r)(1+E(t))+D(1-E(t))}{(\mathrm{Cl}(0)+r)(1-E(t))+D(1+E(t))}\right) - r & \text{if } r > 0, \\ \frac{\mathrm{Cl}(0)}{1+2k_2t\mathrm{Cl}(0)} & \text{if } r = 0. \end{cases} \tag{19}$$

$$\mathrm{Cl_2}(t) = \frac{1}{2}\left(\mathrm{Cl_y} - \mathrm{Cl}(t)\right), \tag{20}$$

where

$$r = \frac{k_1}{4k_2}, \tag{21}$$

$$D = \sqrt{r^2 + 2r\mathrm{Cl_y}}, \tag{22}$$

$$E(t) = e^{-4k_2\mathrm{D}t}. \tag{23}$$

GMDD
7, 8769–8804, 2014

For long times, $\mathrm{Cl}(t)$ and $\mathrm{Cl}_2(t)$ converge to the steady state solutions,

$$\lim_{t\to\infty}\mathrm{Cl}(t) = D - r, \tag{24}$$

$$\lim_{t\to\infty}\mathrm{Cl}_2(t) = \frac{1}{2}\left(\mathrm{Cl_y} - D + r\right), \tag{25}$$

and are shown on Fig. 2. The steady state solutions are specified as initial conditions for the terminator test case. For a stability analysis of the terminator "toy" chemistry see Appendix B.

3 Transport operator and correlations

Let $\mathcal{T}$ be the discrete transport operator that advances, in time, the numerical solution to the passive and inert continuity equation for species Cl and Cl_2

$$\frac{\mathrm{D}\phi}{\mathrm{D}t} = 0, \quad \phi = \mathrm{Cl}, \mathrm{Cl}_2, \tag{26}$$

at grid point or grid cell k:

$$\phi_k^{n+1} = \phi_k^n + \Delta t_{\mathrm{tracer}}\,\mathcal{T}(\phi_j^n), \quad j \in \mathcal{H}, \quad \phi = \mathrm{Cl}, \mathrm{Cl}_2 \tag{27}$$

where n is the time-level index, $\Delta t_{\mathrm{tracer}}$ time-step for the transport operator, and $\mathcal{H}$ is the set of indices defining the stencil required by $\mathcal{T}$ to update ϕ_k^n. Note that the transport operator may not solve the prognostic equation for ϕ in advective form as used in Eqs. (4) and (5). For example, it is common practice for finite-volume schemes to base the discretization on a flux-form formulation of the continuity equation (here written without forcing terms)

$$\frac{\partial(\rho\phi)}{\partial t} = -\nabla\cdot(\boldsymbol{v}\rho\phi), \tag{28}$$

GMDD
7, 8769–8804, 2014

where ρ is air density. To deduce the mixing ratio from Eq. (28) one needs to solve the continuity equation for air. For a non-divergent wind field and an initial condition of ρ that is constant, the exact solution for ρ is that it remains constant in time and space. For the terminator test, in which we use a non-divergent flow field and constant initial condition for ρ (if applicable), it has been found crucial to solve for ρ rather than prescribing the analytic solution for ρ. Usually a transport scheme using $\rho\phi$ as a prognostic variable will not preserve a $\rho\phi$ = constant initial condition whereas it will preserve a constant mixing ratio. So if ρ is analytically prescribed ϕ will not be preserved in areas where it would otherwise be constant. Such errors can be exacerbated by the terminator chemistry. For a fuller discussion of tracer-air coupling see, e.g., Lauritzen et al. (2011) and Nair and Lauritzen (2010).

For the theoretical discussion it is convenient to define the property *semi-linear*: A transport operator $\mathcal{T}$ is semi-linear if it satisfies

$$\mathcal{T}(a\phi_k + b) = a\mathcal{T}(\phi_k) + b\mathcal{T}(1) = a\mathcal{T}(\phi_k) + b, \tag{29}$$

for any constants a and b (Lin and Rood, 1996; Thuburn and McIntyre, 1997). A semi-linear transport operator preserves linear correlation between two trace species. Note that the semi-linear property subsumes that the transport operator preserves a constant mixing ratio

$$\mathcal{T}(b) = b. \tag{30}$$

Since Cl_y is simply the weighted sum of just two species, Cl_y will be conserved in the numerical model if $\mathcal{T}$ is semi-linear. The semi-linear property, however, does not imply that a weighted (linear) sum of more than 2 species is conserved (Lauritzen and Thuburn, 2012). The chemical reactions (Equations 1 and 2), even in discrete form, will preserve the sum of chlorine species. Consequently, a semi-linear transport operator combined with the terminator chemistry will produce no error in Cl_y.

Several transport operators $\mathcal{T}$ in the literature are semi-linear when limiter/filters are not applied. For example, Lin and Rood (1996) show that their scheme, based on

GMDD
7, 8769–8804, 2014

the widely used Piecewise-Parabolic Method (PPM; Colella and Woodward, 1984) for reconstructing sub-grid scale tracer fields, preserves linear correlations. The CSLAM scheme (Lauritzen et al., 2010), also based on polynomials, preserves linear correlations (see proof in Appendix A of Harris et al., 2010). An example of a scheme that is not semi-linear is the transport operator based on rational functions described in Xiao et al. (2002) due to the non-linearity of the reconstruction function.

Typically, transport operators are not applied in their unlimited versions in full models. Shape-preserving filters are applied to ensure physically realizable solutions such as the prevention of negative mixing ratios or unphysical oscillations in the numerical solutions (e.g. Durran, 2010). Perhaps the most widely used limiter in finite-volume schemes is flux-corrected transport (Zalesak, 1979) and/or reconstruction function filters (Colella and Woodward, 1984; Lin and Rood, 1996).

Shape-preserving filters may render an otherwise semi-linear transport operator non-semi-linear. Some limiters, however, are semi-linear. For example, van Leer type 1-D limiters (Lin et al., 1994) preserve linear correlations (Lin and Rood, 1996). Flux-corrected transport limiters with and without selective limiting preserves linear correlations (Blossey and Durran, 2008; Harris et al., 2010). The limiter by Barth and Jespersen (1989), that scales the reconstruction functions so that it is within the range of the surrounding cell average values, preserves linear correlations (Harris et al., 2010). Positive definite limiters that insure positivity-preservation and "clipping" algorithms that simply remove negative values (see, e.g., Skamarock and Weisman, 2009, for applications in a weather forecast model), are certain to violate linear correlations as the filter only affects the species that is about to become negative and not the other species.

4 Discrete terminator test

Coupling the chemistry parameterization with advection can be done in many ways. A common approach in weather/climate modeling is to update the species evolution in time incrementally by first updating the mixing ratios with respect to sub-grid-scale

GMDD
7, 8769–8804, 2014

forcings (referred to as *physics*) and then apply the transport operator based on the physics-updated state (or in reverse order). Since the computation of the sub-grid-scale tendencies in full models is computationally costly, the dynamical core (in this case the transport scheme) is usually subcycled with respect to physics.

Algorithm 1 Pseudo-code explaining the different levels of subcycling and physics-dynamics coupling used in CAM-SE.

Outer loop advances solution Δt in time:
for $t = 1, 2, \ldots$ **do**
  Compute physics tendencies F_i, $i = \mathrm{Cl}, \mathrm{Cl}_2$
  for $ns = 1, 2, \ldots, \mathrm{nsplit}$ **do**
    Update state with chemistry/physics tendencies:
    $C_i = C_i + \frac{\Delta t}{\mathrm{nsplit}} F_i$, $i = \mathrm{Cl}, \mathrm{Cl}_2$
    for $rs = 1, 2, \ldots, \mathrm{rsplit}$ **do**
      subcycling of tracer advection:
      $C_i = C_i + \frac{\Delta t}{\mathrm{nsplit} \times \mathrm{rsplit}} \mathcal{T}(C_i)$, $i = \mathrm{Cl}, \mathrm{Cl}_2$
    end for
  end for
end for

The different levels of subcycling used in CAM-SE are explained via pseudo-code in algorithm 1 using CAM-SE namelist conventions: nsplit and rsplit. The outer time-stepping loop starts with a call to physics that computes the physics tendencies over the entire physics time-step Δt. The full physics tendencies are divided into nsplit adjustments of equal size and in each iteration of the nsplit loop the adjustments are added to the state. The tracer transport scheme may not be stable on the physics time-step (Δt) or the adjustment time-step ($\Delta t/\mathrm{nsplit}$) so it must be subcycled with respect to the physics adjustments. The number of iterations of the tracer transport subcycling

GMDD
7, 8769–8804, 2014

loop is rsplit. Note that since the nsplit and rsplit loops are nested the tracer time-step is $\Delta t_{\text{tracer}} = \Delta t/(\text{nsplit} \times \text{rsplit})$.

We distinguish between the nsplit = 1 and nsplit > 1 configurations and refer to them as ftype = 1 and ftype = 0, respectively, based on CAM-SE namelist terminology (ftype refers to *forcing type*)[1]. CAM-FV uses a ftype = 1 configuration (with the caveat the physics tendencies are added after the transport is complete) and CAM-SE supports both ftype = 0 and ftype = 1. The current default CAM-SE uses ftype = 0.

If the physics time-step is large the ftype = 1 coupling method may produce large physics tendencies that drive the state much out of balance. When the dynamical core is given the physics updated state that is strongly (and locally) out of balance, the dynamical core may produce excessive gravity waves. To alleviate this one may chose to update the state with respect to physics tendencies throughout the tracer subcycling. This approach of adding the physics tendencies as several equal-sized adjustments is the ftype = 0 configuration.

It is, of course, up to the model developer to choose which coupling method is used. To facilitate comparison the model developer is encouraged to use the analytically computed forcing terms F_{Cl} and F_{Cl_2} given in Appendix C, and to use a physics time-step of $\Delta t = 1800\,\text{s}$. The initial conditions are given by the steady state asymptotic solutions Eqs. (24) and (25) with a mixing ratio of $\text{Cl}_y = 4 \times 10^{-6}$ (Fortran code for the initial conditions is given in Appendix D and in the Supplement).

For simplicity the velocity field for the transport operator $\mathcal{T}$ is prescribed. We use the deformational flow of Nair and Lauritzen (Case-2; 2010) that was also used in the standard test case suite of Lauritzen et al. (2012, 2014). For completeness the components of the non-divergent velocity vector $\boldsymbol{V}(\lambda, \theta, t)$ and the stream function are repeated in Appendix A. The test is run for 12 days (or 5 non-dimensional time-units)

[1] when running the 3-D CAM-SE dynamical core nsplit defines the vertical remapping time-step; if ftype = 0 then nsplit also defines the adjustment time-step whereas if ftype = 1 then nsplit only defines the remapping time-step as the full adjustments are added at the beginning of dynamics only.

GMDD
7, 8769–8804, 2014

exactly as prescribed in Nair and Lauritzen (2010). Note that the test case methodology can be applied in any velocity field including a full 3-D dynamical core.

5 Results

It is the purpose of this section to show exploratory terminator test results. An in-depth analysis of why the limiters do not preserve linear relations (and the derivation of possible remedies) is up to the scheme developers.

5.1 Model setup

Terminator test results are shown for two dynamical cores (transport schemes) available in the CAM: CAM-FV (Lin, 2004) and CAM-SE (Dennis et al., 2012) that are documented within the framework of CAM in Neale et al. (2010). The transport scheme in CAM-FV is the widely used finite-volume scheme of Lin and Rood (1996). CAM-SE performs tracer transport using the spectral element method based on degree three polynomials. Further details on CAM-SE are given in Appendix E.

As discussed in detail in Nair and Lauritzen (2010) and briefly in Sect. 3, care must be taken in the handling of tracer mixing ratio and tracer mass coupling for schemes that prognose tracer mass. In general the transport scheme will not preserve a constant mass field ($\rho\phi$ = constant) since the discrete divergence operator is non-zero despite the analytical wind field being non-divergent (zero divergence). However, the scheme will preserve a constant mixing ratio if q is recovered from $\rho\phi$ by diving the tracer mass with the prognosed density ρ. If one does not prognose ρ and simply specify the analytic solution (ρ = constant), a constant mixing ratio will not be preserved.

For all simulations the physics time-step is $\Delta t = 1800\,\mathrm{s}$. The horizontal resolution is approximately 1°: For CAM-FV that is the 0.9×1.25 configuration (192 latitudes and 288 longitudes) and for CAM-SE it is the NE30NP4 configuration in which there are 30×30 elements on each cubed-sphere panel and 4×4 Gauss–Lobatto–Legendre

GMDD
7, 8769–8804, 2014

(GLL) quadrature points in each element. The tracer time step Δt_{tracer} is 900 s for CAM-FV and 300 s for CAM-SE. During the tracer transport scheme time-step the analytic winds of Nair and Lauritzen (2010) are held constant following the CAM-Chem setup (Lamarque et al., 2012).

The physics-dynamics coupling in the current default CAM-SE is ftype = 0 in which the total physics tendency is divided into nsplit chunks. For the 1° setup (NE30NP4) we use the standard/recommended configuration with rsplit = 3 and nsplit = 2 (see pseudo-code in algorithm 1) so that for every third tracer time-step half of the physics tendencies are added to the state. CAM-FV uses ftype = 1 configuration where the physics tendencies are added once[2].

The sample results shown next are divided into four sections. First of all baseline results for CAM-FV and CAM-SE using their default configurations. Next results from experiments varying the limiter in CAM-SE are presented. Then the consequences of using different physics-dynamics coupling methods (in CAM-SE) are discussed. Last the results are quantified.

5.2 Default CAM-FV and default CAM-SE results

Figure 3 shows the distributions Cl_y after 1 and 6 simulated days for CAM-FV and CAM-SE. Ideally Cl_y should be conserved. Both CAM-FV and CAM-SE show deviations from constancy in Cl_y (note that the color-scale on the Figures is not linear). The errors in Cl_y are produced at the terminator when the limiter is most challenged. After the errors are introduced they propagate away from the terminator following Lagrangian trajectories of the prescribed flow. This is most visible for CAM-SE at day 6 (see Fig. 3 and/or animations in Supplement).

CAM-FV transport is based on the dimensionally split Lin and Rood (1996) scheme. The scheme produces errors in Cl_y since the limiter used in CAM-FV (described in

[2]Note, however, that in CAM-FV the tendencies are added after tracer transport and not before

GMDD
7, 8769–8804, 2014

Appendix B of Lin, 2004) does not strictly conserve linear relations. The errors appear to be largest when the flow is aligned with the terminator at a 45° angle (see animation in Supplement). In that situation the dimensionally split approach is most challenged; the shape-preserving limiter is not strictly shape-preserving in the cross direction since the one-dimensional limiters are only applied in the coordinate directions (Lauritzen, 2007).

CAM-SE does not preserve linear relations either and the errors in Cl_y are about an order of magnitude larger than CAM-FV. The CAM-SE limiter is optimization-based (using least-squares) and guarantees no under- or over-shoots at the element level while not violating mass-conservation (Guba et al., 2014). While the optimization based limiter should theoretically preserve linear relations, its present implementation in CAM-SE does not lead to such preservation. It is likely that this behavior is associated with a flow across a stationary discontinuity maintained by the chemistry. This is in contrast to the more standard initial state discontinuity commonly used in inert tracer advection tests (slotted cylinder test 4 in Lauritzen et al., 2012), where tests show the limiter does preserve linear correlations to near round-off.

5.3 CAM-SE: limiter experiments

In addition to the quasi-monotone mass-conservative limiter used by default in CAM-SE, the model has options for performing tracer advection without any limiter and with a positive definite limiter. Results for terminator test runs using those configurations are shown on Fig. 4. As expected the unlimited version of the CAM-SE transport exactly preserves linear relations i.e. Cl_y is conserved to machine precision. By looking at cross sections of the individual distributions of Cl and Cl_2 on Fig. 5, it is immediately apparent (and expected) that Gibbs phenomena manifests itself near the terminator when no limiter is used. The stability analysis discussed in Appendix B and illustrated in Figs. B1 and B2 indicates that the terminator chemistry will drive a negative mixing ratio even more negative. From the experiments, however, the amplitude of the spurious oscillations near the terminator remain nearly constant in time. In other words, the

GMDD
7, 8769–8804, 2014

instability associated with negative mixing ratios in the terminator chemistry is weak in our present setup.

When using a positive definite limiter Gibbs phenomena is eliminated near the base of the terminator but not near the maximum. This obviously violates linear relations and produces large errors in Cl_y. Similar results are expected from mass-filling algorithms in which negative values are simply set to zero. This emphasizes the importance of using carefully designed limiters in transport schemes used for applications in which preservation of linear pre-existing relations is important, e.g., chemistry applications (for a fuller discussion see, e.g., Lauritzen and Thuburn, 2012).

5.4 CAM-SE: Physics-dynamics coupling experiments

As explained in Sect. 4 the dynamics (tracer transport) and physical parameterizations (terminator chemistry) can be coupled in various ways. Here we discuss results based on two coupling methods available in CAM-SE referred to as ftype = 1 and ftype = 0. In ftype = 1 the tendencies from physics are added to the atmospheric state at the beginning of dynamics. For ftype = 0 the tendencies are split into nsplit equal-sized adjustments. On Fig. 6 the total chlorine Cl_y is shown using the ftype = 1 configuration, ftype = 0 using nsplit = 2 and nsplit = 6, respectively. In all experiments the tracer time-step is held fixed so in the latter two configurations rsplit = 3 and rsplit = 1, respectively.

Near the western edge of the terminator (located at approximately 130° W on Fig. 5) where the gradients are steepest, the errors in Cl_y are largest for ftype = 1. The physics adjustments that steepen the gradients are largest at the western edge and consequently produces states that challenges the limiters more. When the physics tendency is added gradually throughout the tracer transport the errors are reduced as nsplit is increased.

At the eastern edge of the terminator (located at approximately 30° E on Fig. 5) the gradients are less steep compared to the western edge. In fact, the location of the gradient near the eastern edge propagates (see animation in Supplement) whereas the gradients at the western edge of the terminator are static in space. The physics

GMDD
7, 8769–8804, 2014

tendencies in this area are not stationary in space and are weaker so the transport signal is larger. This means that for any given point in the eastern area, the state used for computing the physics tendencies changes during the tracer subcycling. As a result the gradients will have propagated during the transport step but the physics tendencies will steepen gradients in the "old" location. This "inconsistency" is present with ftype = 0. For ftype = 1 the physics update is based on the "correct" in time state. The temporal inconsistency in the state used for computing physics tendencies for ftype = 0 produces an increase in errors near the eastern edge of the terminator compared to ftype = 1.

Physical parameterization packages may contain code that sets negative mixing ratios to zero. Or similarly there may be code that prevent tendencies to be added to the state if it is zero or negative. The terminator test may be a useful tool to diagnose such alternations in large complicated codes.

5.5 Quantification of Cl_y errors

To quantify the errors introduced in the terminator test, we suggest to compute standard error norms for Cl_y. The global normalized error norms used are $\ell_2(t)$ and $\ell_\infty(t)$ (e.g., Williamson et al., 1992):

$$\ell_2(t) = \sqrt{\frac{I[(Cl_y(t) - Cl_y(0))^2]}{I[(Cl_y(0))^2]}}, \tag{31}$$

$$\ell_\infty = \frac{\max_{\forall\lambda,\theta}|Cl_y(t) - Cl_y(0)|}{\max_{\forall\lambda,\theta}|Cl_y(0)|}, \tag{32}$$

GMDD
7, 8769–8804, 2014

where $Cl_y(0) = 4 \times 10^{-6}$ is the globally-uniform initial condition and the global integral I is defined as follows,

$$I(\phi) = \frac{1}{4\pi} \int_0^{2\pi} \int_{-\pi/2}^{\pi/2} \phi(\lambda, \theta, t) \cos\theta \mathrm{d}\lambda \mathrm{d}\theta. \quad (33)$$

As a reference we show the time-evolution of $\ell_2(t)$ and $\ell_\infty(t)$ for CAM-FV and CAM-SE on Fig. 7.

6 Conclusions

A simple idealized "toy" chemistry test case is proposed. It consists of advecting two reactive species (Cl and Cl_2) in the Nair and Lauritzen (2010) flow field. The simplified non-linear chemistry creates strong gradients in the species similar to what is observed for photolysis driven species in the stratosphere. The forcing terms for the continuity equations for Cl and Cl_2 are computed analytically over one time-step (assuming no advection) and Fortran codes for computing the forcing terms are provided as Supplement. Hence, model developers who have already setup the standard test case suite of Lauritzen et al. (2012) can with modest efforts setup the terminator test by adding the forcing terms to their codes. As the test case of Nair and Lauritzen (2010) this forced advection problem has an analytic solution.

The "toy" chemistry by design does not disrupt pre-existing linear relations between the species. So the only source of error is from the transport scheme and/or the physics-dynamics coupling. The terminator test is setup so that Cl_y is a constant so any deviation from constancy is an error in preserving linear correlations. Many transport schemes preserve linear relations when no shape-preserving limiter/filter is applied and are therefore not challenged with respect to conserving Cl_y. However, many shape-preserving limiters/filters render the transport scheme non-conserving with respect to Cl_y. While preservation of linear correlations can indeed be verified in inert

GMDD
7, 8769–8804, 2014

advection setup, the terminator chemistry exacerbates the problem through the constant forcing that creates very steep gradients. It is demonstrated in this paper that the terminator test is useful for challenging the limiters with strong grid-scale forcing. In particular, it is shown that positive definite limiters severely disrupt linear correlations near the terminator.

Another application is to use the terminator test for assessing the accuracy of physics-dynamics coupling methods in an idealized setup. It is shown that different coupling methods (such as those available in CAM-SE) lead to different distributions of Cl_y. Also, physics-dynamics coupling layer or the physical parameterization package may contain code that sets negative mixing ratios to zero and/or contain if-statements that prevent tendencies to be added to the state if it is zero or negative. The terminator test may be a useful tool to diagnose such alternations in large complicated codes.

The terminator test is easily accessible to advection scheme developers from an implementation perspective since the software engineering associated with extensive parameterization packages is avoided. The test forces the model developer to consider how their scheme is coupled to sub-grid scale parameterizations and, if solving the continuity equation in flux-form, forces the developer to consider tracer-mass coupling. Also, the idealized forcing proposed here has an analytic formulation and the continuous set of forced transport equations have, contrary to the Brusselator forcing, an analytic solution for the weighted sum of the correlated species irrespective of the flow field.

We encourage dynamical core developers to implement the toy chemistry in their test suite as it has the potential to identify tracer transport issues that standard tests (with unreactive/inert tracers) would not generate.

Appendix A: Idealized flow field

In the terminator test we use the deformational flow of Nair and Lauritzen (Case-2; 2010). The components of the non-divergent velocity vector $\mathbf{V}(\lambda, \theta, t)$ and the stream

GMDD
7, 8769–8804, 2014

function

$$u = -\frac{\partial \psi}{\partial \theta}, \tag{A1}$$

$$v = \frac{1}{\cos\theta}\frac{\partial \psi}{\partial \lambda}, \tag{A2}$$

are given by

$$u(\lambda,\theta,t) = \frac{10R}{T}\sin^2(\lambda')\sin(2\theta)\cos\left(\frac{\pi t}{T}\right) + \frac{2\pi R}{T}\cos(\theta) \tag{A3}$$

$$v(\lambda,\theta,t) = \frac{10R}{T}\sin(2\lambda')\cos(\theta)\cos\left(\frac{\pi t}{T}\right), \tag{A4}$$

$$\psi(\lambda,\theta,t) = \frac{10R}{T}\sin^2(\lambda')\cos^2(\theta)\cos\left(\frac{\pi t}{T}\right) - \frac{2\pi R}{T}\sin(\theta), \tag{A5}$$

respectively, where λ is longitude, θ is latitude, t is time and the underlying solid-body rotation is added through the translation $\lambda' = \lambda - 2\pi t/T$. The period of the flow is $T = 12$ days and $R = 6.3172 \times 10^6$ m (in non-dimensional units $T = 5$ and $R = 1$). Schemes based on characteristics, e.g. Lagrangian and semi-Lagrangian schemes, may use the semi-analytic trajectory formulas given in (Nair and Lauritzen, 2010). Note that it is not necessary to use an analytic flow field for this test case setup. In fact, one may use winds from a weather or climate model simulation.

Appendix B: Stability of chemical kinetics

Relation Eq. (16) is plotted in Figs. B1 and B2. As can be seen in Fig. B1, for $k_1 > 0$, Cl converges to $D - r$. For $k_1 = 0$ Fig. B2 shows that Cl converges to zero for values greater

GMDD
7, 8769–8804, 2014

than zero, but diverges for Cl < 0. While Cl should never be negative, numerical errors can lead to negative values. This divergence is slow, in the sense that the divergence is algebraic as can be seen in Eq. (19). The divergence is also slow in the sense that the time required to double a negative Cl concentration is

$$t_2 = -\frac{1}{4k_2\mathrm{Cl}}. \tag{B1}$$

Thus, for very small (negative) Cl, the time will have to be particularly large. However, for time of $2 \cdot t_2$, the solution is singular, reaching a value of $-\infty$.

Appendix C: Analytic chemical forcing term

The analytic solution of the equations leads to an explicit solution for the change in concentrations during a time step with no flow.

$$F^n_{\mathrm{Cl}} = -L_{\Delta t}\frac{(\mathrm{Cl}^n - D + r)(\mathrm{Cl}^n + D + r)}{1 + E(\Delta t) + \Delta t L_{\Delta t}(\mathrm{Cl}^n + r)}. \tag{C1}$$

where Cl^n is the value of Cl at the beginning of the n'th time step,

$$L_{\Delta t} = \begin{cases} \frac{1-e^{-4k_2 D\Delta t}}{D\Delta t} & \text{if } D > 0 \\ 4k_2 & \text{if } D = 0. \end{cases} \tag{C2}$$

and by conservation,

$$F^n_{\mathrm{Cl}_2} = -\frac{1}{2}F^n_{\mathrm{Cl}}. \tag{C3}$$

In implementation, $L_{\Delta t}$ needs some care. As $4k_2 D\Delta t$ approaches machine precision, it is useful to simply use the formula for $D = 0$ rather than the expression for $D > 0$.

GMDD
7, 8769–8804, 2014

Appendix D: Fortran code

In terms of Fortran code the analytical forcing is given by:

```
! dt is size of physics time step
cly = cl + 2.0*cl2

r = k1/(4.0*k2)
d = sqrt(r*r + 2.0*r*cly)
e = exp(-4.0*k2*d*dt)

if(abs(d*k2*dt).gt. 1e-16)
  el = (1.0-e)/(d*dt)
else
  el = 4.0*k2
endif

f_cl  = -el * (cl-d+r) * (cl+d+r)/(1.0 + e + dt*el*(cl+r))
f_cl2 = -f_cl/2.0
```

The reaction rates are defined by

```
! k1 and k2 are reaction rates
k1_lat_center =  20.0 ! degrees
k1_lon_center = 300.0 ! degrees
k1 = max(0.d0,
         sin(lat)*sin(k1_lat_center)
         + cos(lat)*cos(k1_lat_center)
           *cos(lon-k1_lon_center))
k2 = 1.0
```


GMDD
7, 8769–8804, 2014

The initial condition is defined by

```
cly = 4.0e-6

r = k1/(4.0*k2)
d = sqrt(r*r + 2.0*cly*r)

cl = d-r
cl2 = cly/2.0 - (d-r)/2.0
```

These specifications are implemented in Fortran code in the Supplement.

Appendix E: CAM-SE time-stepping

The tracer algorithm and dynamical core use the same time step which is controlled by the maximum anticipated wind speed, but the dynamics uses more stages of a second-order accurate N-stage Runge–Kutta (RK) method in order to maintain stability. CAM-SE's tracer advection algorithm is based on a 3-stage RK strong-stability-preserving (SSP) time-stepping method (Spiteri and Ruuth, 2002). The SSP method ensures that the time step will preserve any monotonicity properties preserved by the underlying spatial discretization. CAM-SE uses monotone limiter in its advection scheme coupled with a monotone hyper-viscosity operator (Guba et al., 2014). This option renders the advection scheme second-order. The time-stepping scheme in the dynamical core uses a third-order accurate 5-stage RK method (modified version of Kinnmark and Gray, 1984a, b; P. A. Ullrich, personal communication, 2013) The extra stages are chosen to maximize the stable time step size. We also note that the hyper-diffusion in the dynamical core requires three subcycled iterations for each dynamics time step (in the NE30NP4 configuration).

GMDD
7, 8769–8804, 2014

The Supplement related to this article is available online at doi:10.5194/gmdd-7-8769-2014-supplement.

Acknowledgements. NCAR is sponsored by the National Science Foundation (NSF). Jean-François Lamarque, Andrew Conley and Francis Vitt were partially funded by Department of Energy (DOE) Office of Biological & Environmental Research) under grant number SC0006747. Mark Taylor was supported by the Department of Energy Office of Biological and Environmental Research, work package 12-015335, "Applying Computationally Efficient Schemes for BioGeochemical Cycles". Thanks to Oksana Guba for discussions on the CAM-SE limiter. The authors are grateful to Michael Prather for the many discussions on simplified chemistry.

References

Anderson, J., Toohey, D., and Brune, W.: Free radicals within the Antarctic vortex: the role of CFCs in Antarctic ozone loss, Science, 251, 39–46, doi:10.1126/science.251.4989.39, 1991. 8772

Barth, T. and Jespersen, D.: The design and application of upwind schemes on unstructured meshes, in: Proc. AIAA 27th Aerospace Sciences Meeting, Reno, 1989. 8778

Blossey, P. N. and Durran, D. R.: Selective monotonicity preservation in scalar advection, J. Comput. Phys., 227, 5160–5183, 2008. 8778

Brasseur, G. and Solomon, S.: Aeronomy of the Middle Atmosphere, Springer, 3rd Edn., 2005. 8772

Colella, P. and Woodward, P. R.: The Piecewise Parabolic Method (PPM) for gas-dynamical simulations, J. Comput. Phys., 54, 174–201, 1984. 8778

Dennis, J. M., Edwards, J., Evans, K. J., Guba, O., Lauritzen, P. H., Mirin, A. A., St-Cyr, A., Taylor, M. A., and Worley, P. H.: CAM-SE: A scalable spectral element dynamical core for the Community Atmosphere Model, Int. J. High Perform. C., 26, 74–89, doi:10.1177/1094342011428142, 2012. 8772, 8781

Durran, D.: Numerical Methods for Fluid Dynamics: With Applications to Geophysics, vol. 32 of Texts in Applied Mathematics, Springer, 2nd Edn., 516 pp., 2010. 8778

Guba, O., Taylor, M., and St-Cyr, A.: Optimization-based limiters for the spectral element method, J. Comput. Phys., 267, 176–195, doi:10.1016/j.jcp.2014.02.029, 2014. 8783, 8791

GMDD
7, 8769–8804, 2014

Harris, L. M., Lauritzen, P. H., and Mittal, R.: A flux-form version of the Conservative Semi-Lagrangian Multi-tracer transport scheme (CSLAM) on the cubed sphere grid, J. Comput. Phys., 230, 1215–1237, doi:10.1016/j.jcp.2010.11.001, 2010. 8778

Kinnmark, I. P. and Gray, W. G.: One step integration methods with maximum stability regions, Math. Comput. Simulat., 26, 87–92, doi:10.1016/0378-4754(84)90039-9, 1984a.

Kinnmark, I. P. and Gray, W. G.: One step integration methods of third-fourth order accuracy with large hyperbolic stability limits, Math. Comput. Simulat., 26, 181–188, doi:10.1016/0378-4754(84)90056-9, 1984b.

Kristensen, L., Lenschow, D. H., Gurarie, D., and Jensen, N. O.: A simple model for the vertical transport of reactive species in the convective atmospheric boundary layer, Bound.-Lay. Meteorol., 134, 195–221, doi:10.1007/s10546-009-9443-x, 2010. 8771

Lamarque, J.-F., Emmons, L. K., Hess, P. G., Kinnison, D. E., Tilmes, S., Vitt, F., Heald, C. L., Holland, E. A., Lauritzen, P. H., Neu, J., Orlando, J. J., Rasch, P. J., and Tyndall, G. K.: CAM-chem: description and evaluation of interactive atmospheric chemistry in the Community Earth System Model, Geosci. Model Dev., 5, 369–411, doi:10.5194/gmd-5-369-2012, 2012. 8782

Lauritzen, P. and Thuburn, J.: Evaluating advection/transport schemes using interrelated tracers, scatter plots and numerical mixing diagnostics, Q. J. Roy. Meteor. Soc., 138, 906–918, doi:10.1002/qj.986, 2012. 8770, 8777, 8784

Lauritzen, P. H.: A stability analysis of finite-volume advection schemes permitting long time steps, Mon. Weather Rev., 135, 2658–2673, 2007. 8783

Lauritzen, P. H., Nair, R. D., and Ullrich, P. A.: A conservative semi-Lagrangian multi-tracer transport scheme (CSLAM) on the cubed-sphere grid, J. Comput. Phys., 229, 1401–1424, doi:10.1016/j.jcp.2009.10.036, 2010. 8778

Lauritzen, P. H., Ullrich, P. A., and Nair, R. D.: Atmospheric transport schemes: desirable properties and a semi-Lagrangian view on finite-volume discretizations, in: Numerical Techniques for Global Atmospheric Models, Lecture Notes in Computational Science and Engineering, edited by: Lauritzen, P. H., Nair, R. D., Jablonowski, C., Taylor, M., Springer, 80 pp., 2011. 8777

Lauritzen, P. H., Skamarock, W. C., Prather, M. J., and Taylor, M. A.: A standard test case suite for two-dimensional linear transport on the sphere, Geosci. Model Dev., 5, 887–901, doi:10.5194/gmd-5-887-2012, 2012. 8770, 8780, 8783, 8786

GMDD
7, 8769–8804, 2014

Lauritzen, P. H., Ullrich, P. A., Jablonowski, C., Bosler, P. A., Calhoun, D., Conley, A. J., Enomoto, T., Dong, L., Dubey, S., Guba, O., Hansen, A. B., Kaas, E., Kent, J., Lamarque, J.-F., Prather, M. J., Reinert, D., Shashkin, V. V., Skamarock, W. C., Sørensen, B., Taylor, M. A., and Tolstykh, M. A.: A standard test case suite for two-dimensional linear transport on the sphere: results from a collection of state-of-the-art schemes, Geosci. Model Dev., 7, 105–145, doi:10.5194/gmd-7-105-2014, 2014. 8770, 8780

Lin, S.-J.: A "vertically Lagrangian" finite-volume dynamical core for global models, Mon. Weather Rev., 132, 2293–2307, 2004. 8772, 8781, 8783

Lin, S.-J. and Rood, R. B.: Multidimensional flux-form semi-Lagrangian transport schemes, Mon. Weather Rev., 124, 2046–2070, 1996. 8777, 8778, 8781, 8782

Lin, S.-J., Chao, W. C., Sud, Y. C., and Walker, G. K.: A class of the van Leer-type transport schemes and its application to the moisture transport in a general circulation model, Mon. Weather Rev., 122, 1575–1593, 1994. 8778

Nair, R. D. and Jablonowski, C.: Moving vortices on the sphere: a test case for horizontal advection problems, Mon. Weather Rev., 136, 699–711, 2008. 8770

Nair, R. D. and Lauritzen, P. H.: A class of deformational flow test cases for linear transport problems on the sphere, J. Comput. Phys., 229, 8868–8887, doi:10.1016/j.jcp.2010.08.014, 2010. 8770, 8771, 8772, 8777, 8780, 8781, 8782, 8786, 8787, 8788

Nair, R. D. and Machenhauer, B.: The mass-conservative cell-integrated semi-Lagrangian advection scheme on the sphere, Mon. Weather Rev., 130, 649–667, 2002. 8770

Neale, R. B., Chen, C.-C., Gettelman, A., Lauritzen, P. H., Park, S., Williamson, D. L., Conley, A. J., Garcia, R., Kinnison, D., Lamarque, J.-F., Marsh, D., Mills, M., Smith, A. K., Tilmes, S., Vitt, F., Cameron-Smith, P., Collins, W. D., Iacono, M. J., Easter, R. C., Ghan, S. J., Liu, X., Rasch, P. J., and Taylor, M. A.: Description of the NCAR Community Atmosphere Model (CAM 5.0), NCAR Technical Note, National Center of Atmospheric Research, 2010. 8781

Prigogine, I.: From Being to Becoming: Time and Complexity in the Physical Sciences, W H Freeman & Co, 1981. 8771

Prigogine, I. and Lefever, R.: Symmetry-breaking instabilities in dissipative systems, J. Chem. Phys., 48, 1695–1700, doi:10.1063/1.1668896, 1968. 8771

Pudykiewicz, J. A.: Numerical solution of the reaction-advection–diffusion equation on the sphere, J. Comput. Phys., 213, 358–390, doi:10.1016/j.jcp.2005.08.021, 2006. 8771

GMDD
7, 8769–8804, 2014

Pudykiewicz, J. A.: On numerical solution of the shallow water equations with chemical reactions on icosahedral geodesic grid, J. Comput. Phys., 230, 1956–1991, doi:10.1016/j.jcp.2010.11.045, 2011.
Salawitch, R. J., Canty, T., Müller, R., Santee, M. L., Schofield, R., Stimpfle, R. M., Stroh, F., Toohey, D. W., and Urban, J.: Sect. 3. Workshop Report: The Role of Halogen Chemistry in Polar Stratospheric Ozone Depletion, in: Workshop for an Initiative under the Stratospheric Processes and Their Role in Climate (SPARC) Project of the World Climate Research Programme, June 2008, Cambridge, UK, 2009. 8772
Skamarock, W. C. and Weisman, M. L.: The impact of positive-definite moisture transport on NWP precipitation forecasts, Mon. Weather Rev., 137, 488–494, doi:10.1175/2008MWR2583.1, 2009. 8778
Spiteri, R. and Ruuth, S.: A new class of optimal high-order strong-stability-preserving time discretization methods, SIAM J. Numer. Anal., 40, 469–491, doi:10.1137/S0036142901389025, 2002. 8791
Thuburn, J. and McIntyre, M.: Numerical advection schemes, cross-isentropic random walks, and correlations between chemical species, J. Geophys. Res., 102, 6775–6797, 1997. 8777
Turing, A.: The chemical basis of morphogenesis, Philos. T. R. Soc. Lon. B, 37–72, 1952. 8771
Williamson, D. L., Drake, J. B., Hack, J. J., Jakob, R., and Swarztrauber, P. N.: A standard test set for numerical approximations to the shallow water equations in spherical geometry, J. Comput. Phys., 102, 211–224, 1992. 8770, 8785
Xiao, F., Yabe, T., Peng, X., and Kobayashi, H.: Conservative and oscillation-less atmospheric transport schemes based on rational functions, J. Geophys. Res., 107, 4609, doi:10.1029/2001JD001532, 2002. 8778
Zalesak, S. T.: Fully multidimensional flux-corrected transport algorithms for fluids, J. Comput. Phys., 31, 335–362, 1979. 8778

GMDD
7, 8769–8804, 2014

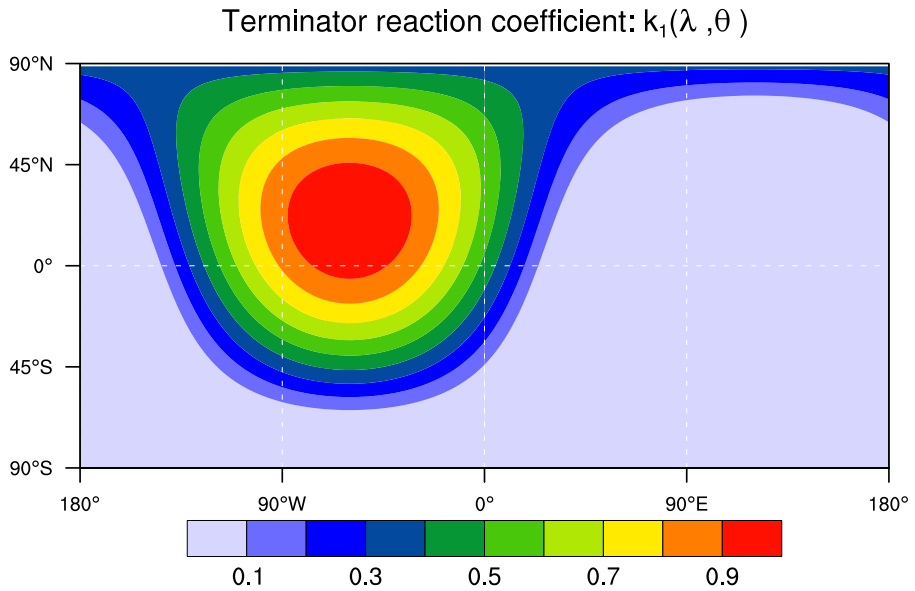

Figure 1. Contour plot of the terminator-"like" reaction coefficient $k_1(\lambda, \theta)$ where λ and θ are longitude and latitude, respectively.

GMDD
7, 8769–8804, 2014

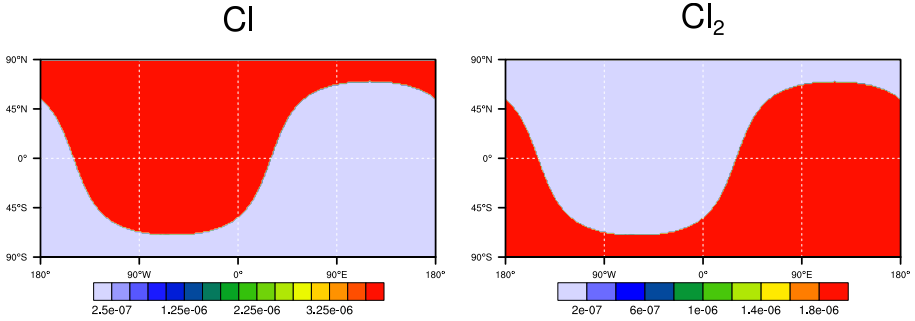

Figure 2. Contour plots of the steady-state solutions, assuming no flow, for Cl (left) and Cl_2 (right), respectively, computed from initial conditions Cl = 4.0×10^{-6} and $Cl_2 = 0$.

GMDD
7, 8769–8804, 2014

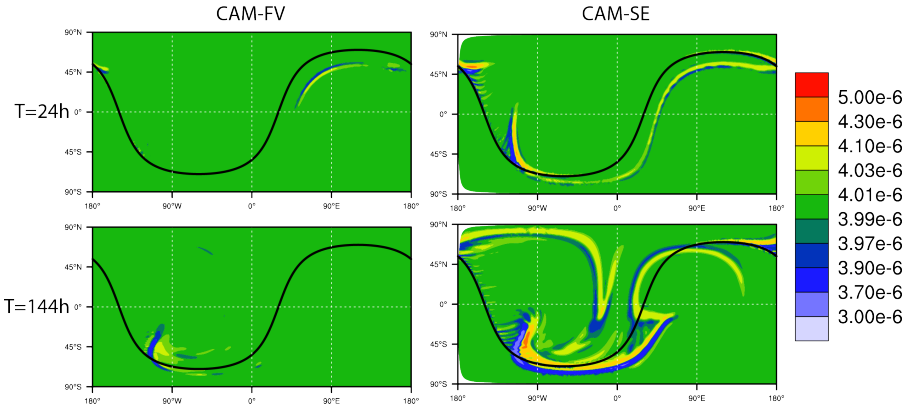

Figure 3. Contour plots of Cl_y for (left column) CAM-FV and for (right column) CAM-SE in ftype = 0 configuration at day 1 (upper row) and day 6 (lower row), respectively. Solid black line is the location of the terminator line. Note that the contour levels are not linear.

GMDD
7, 8769–8804, 2014

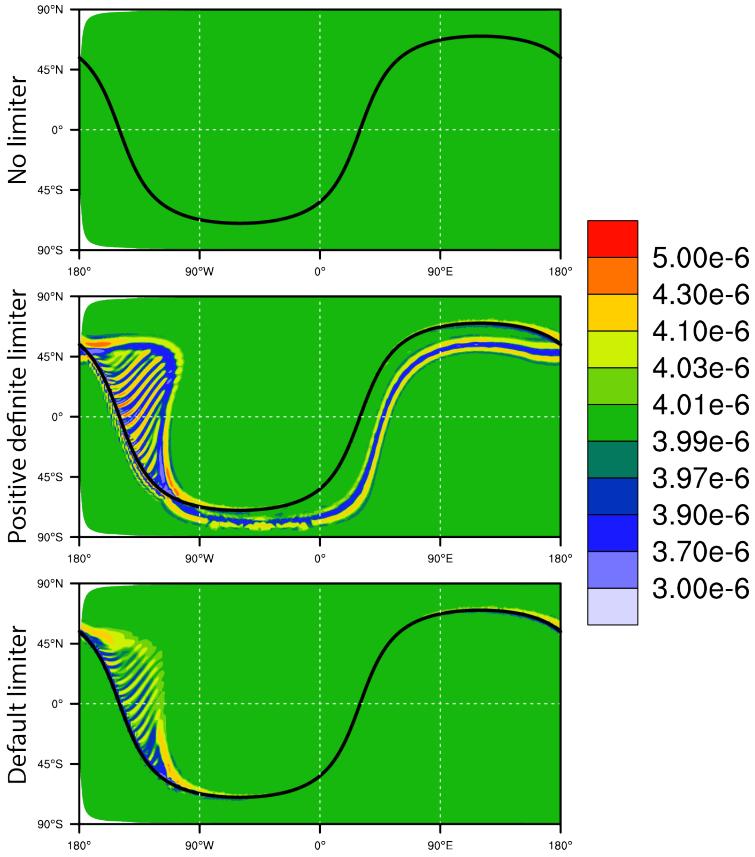

Figure 4. Contour plot of Cl_y at day 1 using CAM-SE in ftype = 1 configuration where (upper) no limiter, (middle) positive definite limiter, and the default CAM-SE limiter is applied, respectively. The solid black line depicts the location of the terminator line. Note that the contour levels are not linear.

GMDD
7, 8769–8804, 2014

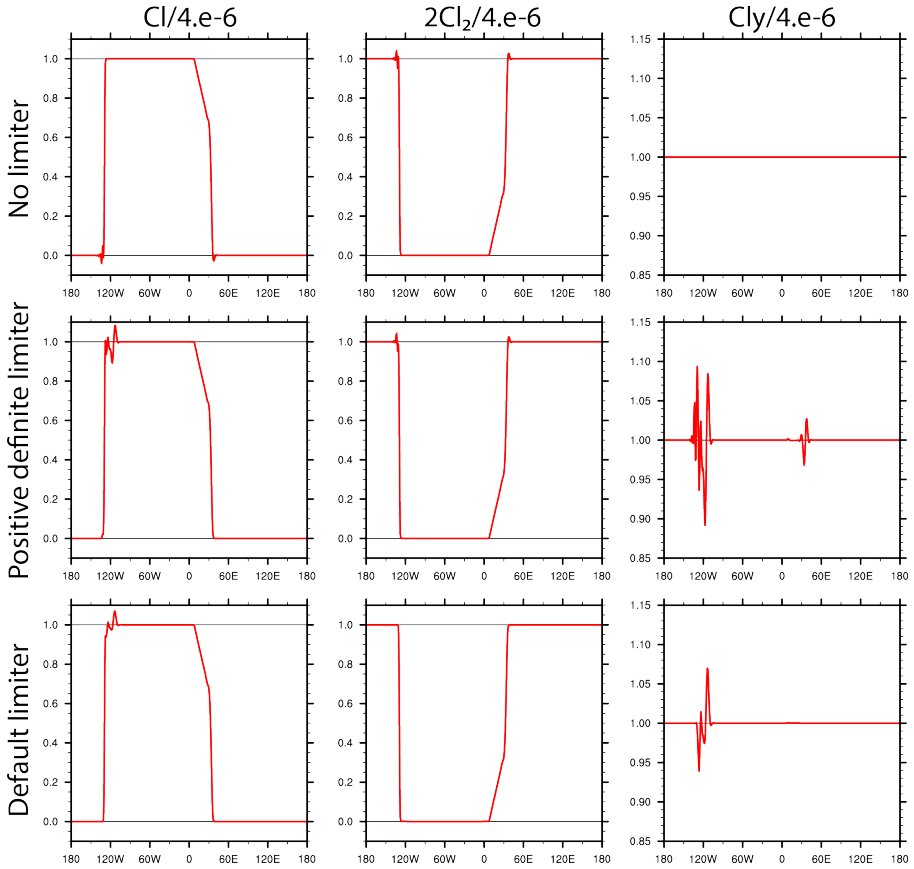

Figure 5. Cross sections of day 1 (left column) Cl, (middle column) $2\times Cl_2$, and (right column) Cl_y at 45° S based on CAM-SE with (top row) no limiter, (middle row) positive definite limiter, (lower row) and default limiter, respectively. Results are normalized by 4×10^{-6} (the initial value of Cl_y).

GMDD
7, 8769–8804, 2014

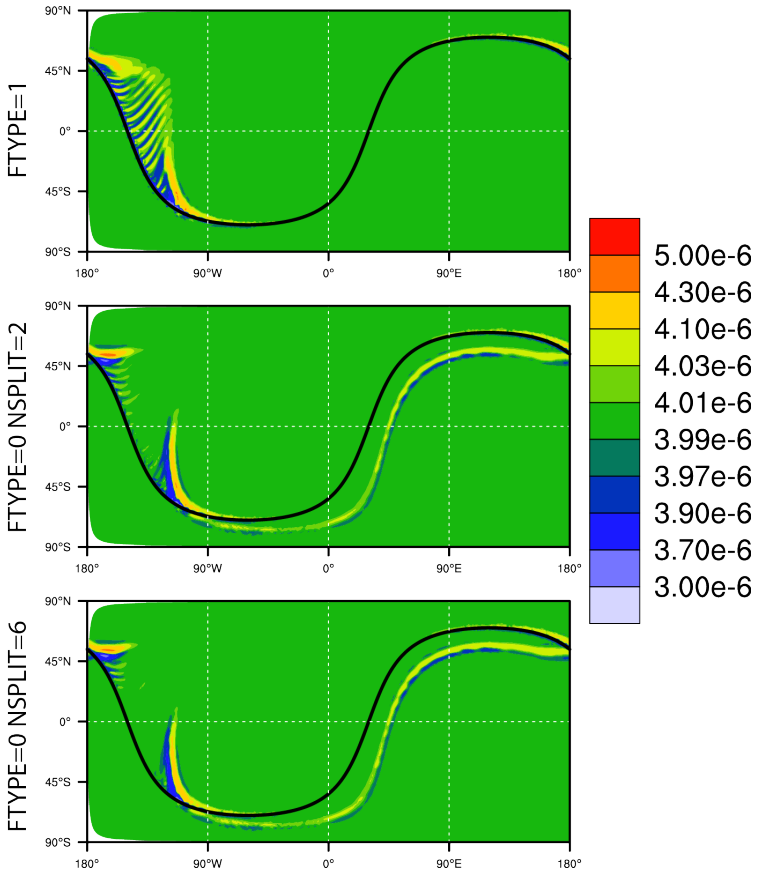

Figure 6. Contour plots of Cl_y at day 1 using CAM-SE based on (upper) ftype = 1, (middle) ftype = 0 and nsplit = 3, and (lower) ftype = 0 and nsplit = 6, respectively. In all simulations the tracer time-step is constant Δt_{tracer} = 300 s.

GMDD
7, 8769–8804, 2014

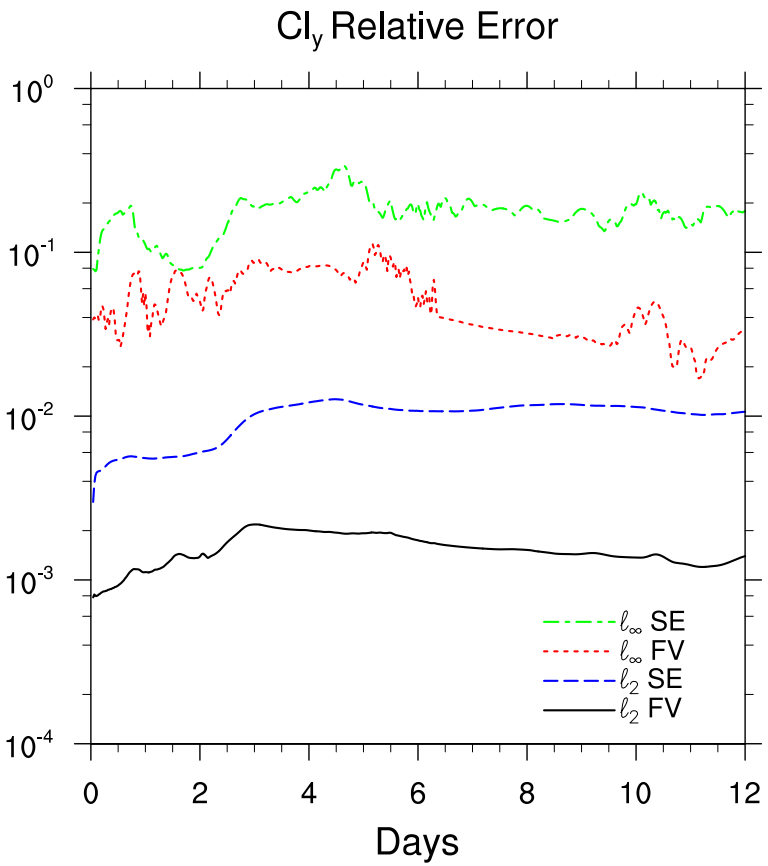

Figure 7. Time-evolution of standard error norms ℓ_2 and ℓ_∞ for Cl_y using CAM-FV and CAM-SE dynamical cores. Note that the y axis is logarithmic.

GMDD
7, 8769–8804, 2014

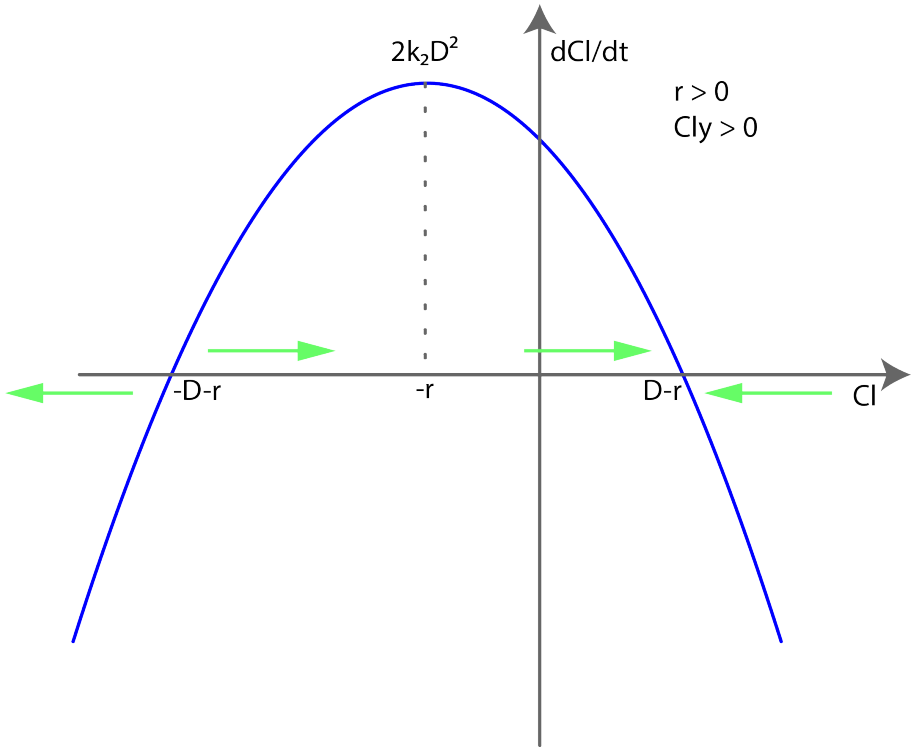

Figure B1. When $k_1 > 0$, or equivilently $r > 0$, there is a single stable limit point. Cl will converge to $D - r$ as long as Cl > $-D - r$.

GMDD
7, 8769–8804, 2014

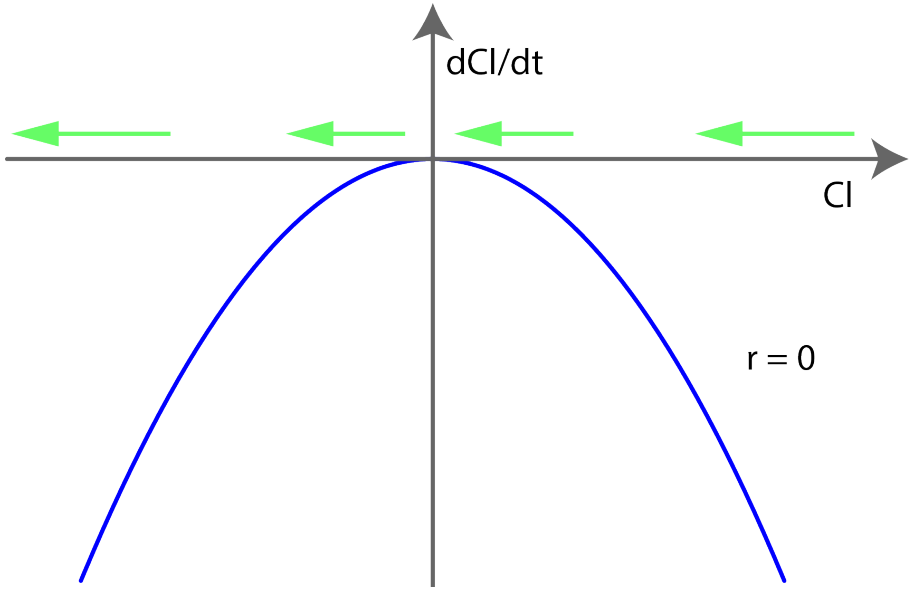

Figure B2. When $k_1 = 0$, or equivilently $r = 0$, Cl converges to zero, but if, for some numerical reason, Cl is driven negative, the kinetic equations will drive the concentrations even more negative.

GMDD
7, 8769–8804, 2014